AIAA'83

AIAA-83-0075

Calorimetric Measurements of Thermal Control Surfaces on Operational Satellites

J.E. Ahern and K. Karperos, Aerojet ElectroSystems Co., Azusa, CA

AIAA 21st Aerospace Sciences Meeting

January 10-13, 1983/Reno, Nevada

CALORIMETRIC MEASUREMENTS OF THERMAL CONTROL SURFACES ON OPERATIONAL SATELLITES

A83-16505

John E. Ahern* and Kurt Karperos**
Aerojet ElectroSystems Company
Azusa, CA

Abstract

The results of flight temperature measurements for a variety of thermal control surfaces on long-life operational satellites in geosynchronous orbit are presented. Solar absorptance values were developed from calorimetric measurements as a function of equivalent sun hours of exposure for second surface mirrors, silvered and aluminized FEP Teflon, white paint, silica cloth, and a silver-alumina-silica surface. Solar absorptance values are presented in the form of curves and exponential equations for up to 10,000 hours of equivalent sun exposure. The dependence of solar absorptance degradation upon time and thermal control surface material is demonstrated.

Nomenclature

a	= Albedo
nm	= Nanometer
t	= Time
A	= Area
C	= Capacitance
F_a	= View Factor, Albedo
F_e	= View Factor, Earthshine
H_e	= Earthshine Heat Rate
S_o	= Solar Heat Flux
T	= Temperature
α_s	= Solar Absorptance
β	= Angle between satellite axis and earth sun plane
ϵ	= Emissivity
θ	= Angle between surface normal and sun vector
σ	= Stefan-Boltzmann constant
τ	= Time constant

1.0 Introduction

It is apparent from many recent papers that the general warming trend with time of orbiting satellite systems is due to degradation of the thermal control surfaces.[1,2,3] In view of the economic benefit derived from reliable long-life satellite operation the design of certain thermal control systems should consider the impact of this time-dependent parameter. A primary aspect of the thermal design for long life is the lack of reliable data on thermal control surfaces exposed to the real space environment. Data that are available consist of two types. The first is developed from temperature measurements made on operational thermal control surfaces and other components that contribute to the heat input and output of the measured radiator surface. The reliability of the performance evaluation of the thermal control surface is dependent to a significant degree on the complexity of the system and the sophistication of of the thermal modeling. Because of the influence of the other components in the system and the usually limited temperature measurements available on spacecraft, this type of data must be considered to be approximate when considering it for use in designing other types of systems. The second type is that developed from calorimeters where the thermal control surface under study is thermally isolated from potential input and output heat flows except those involving solar heating and space heat rejection. In this latter approach the test sample temperature provides a direct indication of the $\alpha s/\epsilon$ value when exposed to solar radiation and of the ϵ value when the sample is shaded from solar input. This paper presents results of orbital flight measurements made using the latter calorimetric method. The data presented includes measurements of solar absorptance as a function of equivalent sun hours of exposure so as to be directly applicable to design purposes. Laboratory measurements of emissivity as a function of temperature are given for some thermal control surfaces. Flight data indicates that emissivity of these thermal control surfaces does not change with time.

The data presented in this report is a continuation of that in Reference 1. The phase II calorimeter described in Reference 1, and shown in Figure 1, was used to obtain the present data. It was installed on several spacecraft in the same clean location (-T axis of Reference 1 satellite) in similar geosynchronous orbits. Each calorimeter had four surface samples one of which was a reference sample to provide direct correlation between the calorimeter results on the different spacecraft. Twenty samples were evaluated on five calorimeters. The samples are listed and described in Table 1.

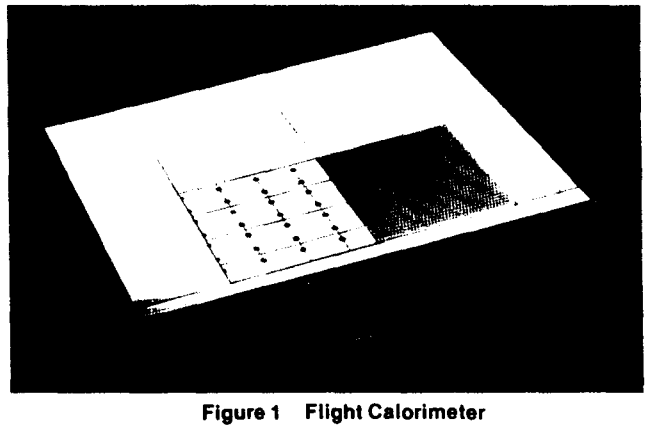

Figure 1 Flight Calorimeter

In the next section the calorimeter design is described including a description of the computer model for data reduction and an error analysis. This is followed by a discussion of the flight measurements with comparisons between the different types of surfaces. The data are developed into equation form as a function of equivalent sun hours for design application. Comparison of the results are made with other data from the literature.

*Senior Technical Specialist, Member AIAA
**Member Technical Staff

Table 1 Calorimeter Sample Description

Flight Sample	Method of Application	Flight Sample	Method of Application
1. 0.002-in Silvered Teflon	Nickel powder filled acrylic adhesive	11. Second Surface Mirror	RTV-566 adhesive
2. 0.005-in Aluminized Teflon	Nickel powder filled acrylic adhesive	12. ZOT paint (8-10 mil thick)*	On AZ31B magnesium
3. Silica cloth No. 581	Heat laminated to 0.001 in aluminized Teflon	13. Second Surface Mirror	RTV-566 adhesive
4. Silica cloth No. 581	Double faced tape with No. 585	14. ZOT paint (10-12 mil thick)*	On 6061-T6 aluminum
5. 0.002-in Silvered Teflon	Nickel powder filled acrylic adhesive	15. Second Surface Mirror	RTV-566 adhesive
6. Indium Oxide Front Coated Mirror	RTV-566 adhesive	16. ZOT paint (6-7 mil thick)*	On 6061-T6 aluminum
7. 0.005-in Embossed Silvered Teflon	With pressure sensitive P/223 tape	17. Silver-Alumina-Silica	Vapor deposited on aluminum (Table 4)
8. Second Surface Mirror	RTV-566 adhesive	18. ZOT paint (10-12 mil thick)*	On 6061-T6 aluminum
9. ZOT paint (8-10 mil thick)*	On 6061-T6 aluminum	19. Second Surface Mirror	RTV-566 adhesive
10. ZOT paint (8-10 mil thick)*	On 6061-T6 aluminum	20. ZOT paint (10-12 thick)*	On AZ31B magnesium

*Zinc orthotitanate pigment in potassium silicate binder YB-71 manufactured by IITRI [10]

2.0 Calorimeter Design And Analysis

2.1 Calorimeter Design

The calorimeter used in this program is shown in the photograph, Figure 1, and a cross-section showing the general construction features is presented in Figure 2. The basic design approach for the calorimeter was directed to maximizing the thermal isolation of the thermal control surfaces under test. This involved using minimum thickness, low-thermal-conducting fiberglass supports, multilayer insulation and reflective aluminized surfaces. Further, the calorimeter was installed in a location chosen to minimize radiant heat transfer between the calorimeter samples and spacecraft external surfaces. A total view factor from calorimeter samples to spacecraft external surfaces of less than 2% was achieved. Finally, the design was configured to avoid complexity in computer thermal modeling so that reliable data evaluation could be achieved. Five calorimeters of this design were flown with no indication of structural failure since all temperature monitors operated throughout their life and the performance of similar reference samples on the different flights matched well. Figures 3 and 4 show the comparison between the reference samples from the five flight calorimeters.

2.2 Calorimeter Analysis

The node locations and the description of the nodes are given in Figure 2 while Figure 5 shows a typical thermal network for one specimen. Several of the nodes are external surfaces of the spacecraft that have a view of the test samples. The radiation coupling between the calorimeter samples and the spacecraft surfaces were obtained using an Aerojet-developed Monte Carlo program. Since the temperatures of these spacecraft surfaces were inputted in the computer program, only the IR radiation between the surfaces and the test samples was involved. Solar heating of the test samples was considered in the computer model by a diurnal shape factor table that was adjustable for β angle and solar heat flux automatically.

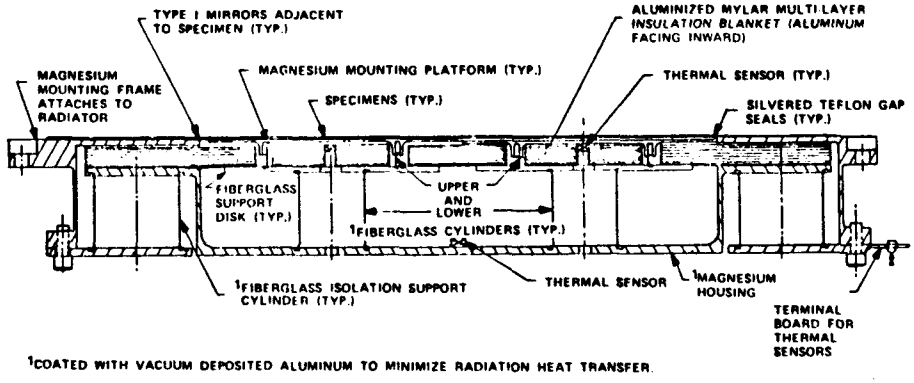

Figure 2 Cutaway View of Calorimeter Design

A flow chart detailing the algorithm by which the solar absorptance values of the flight test samples were evaluated is given in Figure 6. For the day of evaluation the diurnal temperatures (available at 15 minute intervals) for the radiation linked spacecraft nodes and the calorimeter base node are inputted into the program. The previously calculated value of the solar absorptance (or an estimated value) for each test sample is entered into the computer program and the corresponding sample temperature diurnals are calculated. As noted in the flow chart, Figure 6, the calculated maximum temperature for each test sample is compared to the actual maximum flight temperatures that were inputted in the computer program. The computer will make adjustments to the solar absorptance values accordingly and iterate until the calculated temperature for the adjusted solar absorptance values matches the flight data within $0.1^{o}F$ thus giving the solar absorptance value for that day.

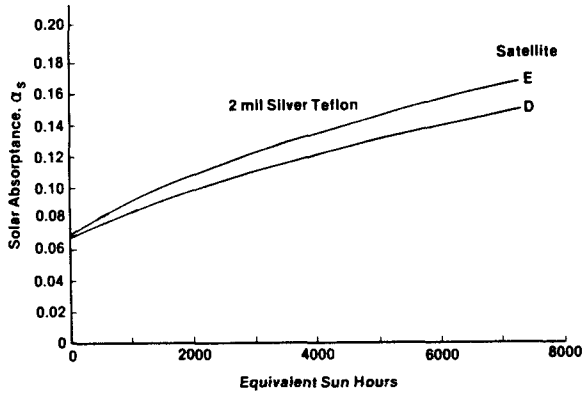

Figure 3 Comparison of Flight Reference Samples, Satellites D and E

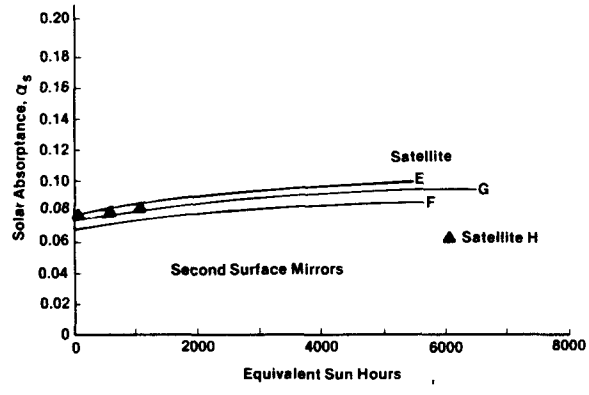

Figure 4 Comparison of Flight Reference Samples, Satellites E F G and H

The analysis of the calorimeter sample performance was done at varying intervals. In general, the time span between data reduction days was determined by the temperature rise rate since the accuracy of determining the solar absorptance value is strongly dependent on the telemetry count error as discussed later. In most cases the solar absorptance rise rates followed a roll-off trend so that early data were obtained at small time intervals on the order of one month and increased with time so that at three years data was taken at approximately 3 month intervals.

The data in this paper are given as a function of equivalent sun hours so direct design applications can be made. It also simplifies the comparison of this flight data with other flight and laboratory data when they are given as a function of equivalent sun hours. An exponential least-square curve fit for each sample material is made for values of solar absortance versus equivalent sun hours allowing easy insertion into thermal design computer programs.

During the process of reducing the flight data errors are introduced that must be considered in the application of the design data.

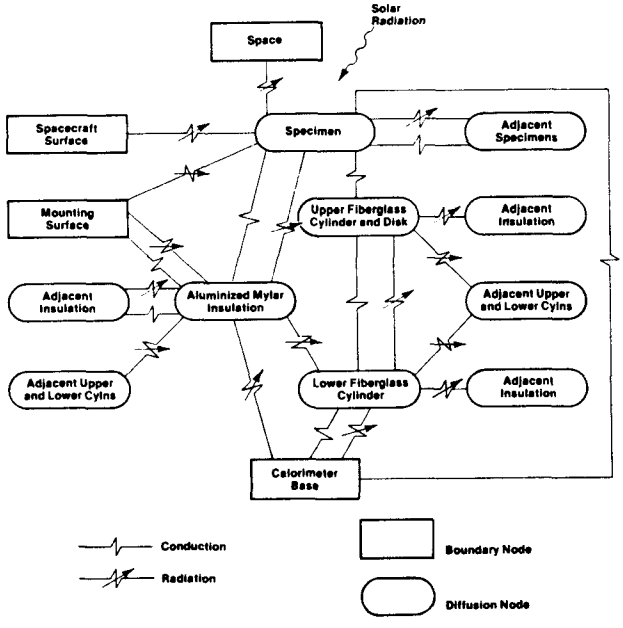

Figure 5 Calorimeter Thermal Network For One Specimen (Typical)

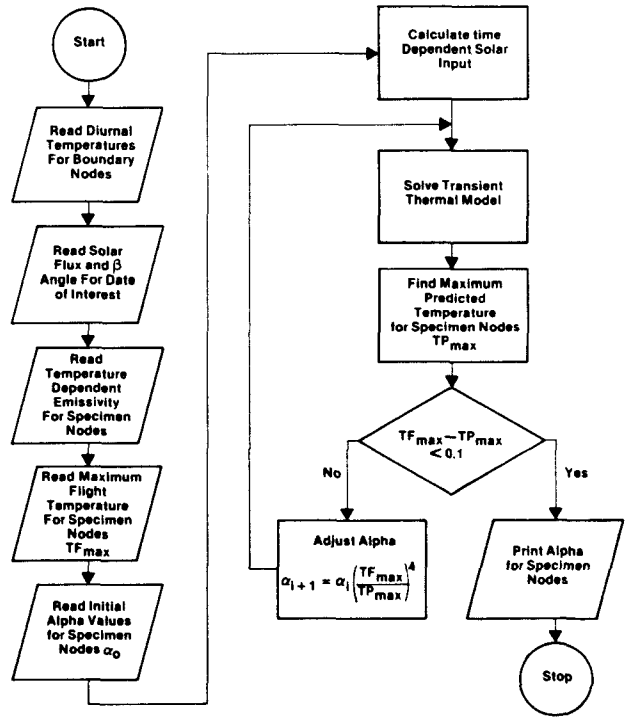

Figure 6 Computer Model Flow Chart

2.3 Error Analysis

The potential sources of errors in developing the solar absorptance values from flight temperature measurements are given in Table 2 along with the uncertainty associated with the source and the error impact on the results.

The three primary sources of error are in the calorimeter design, the temperature monitor calibration, and the telemetry quantization. The measurement of absolute solar absorptance involves the full calorimeter design errors, the temperature monitor calibration error, and the telemetry quantization error. As noted in Table 2 the estimated error for measuring the absolute solar absorptance is +0.009, -0.006. The actual initial flight measured values of α_s for all 20 samples are listed in Table 3 and compared to the laboratory values measured before flight. Except for two zinc orthotitante (ZOT) paint samples and one silica cloth sample all the flight measurements match the laboratory value within the error band. A general conclusion can be made from these results that the ground handling and launch conditions did not contribute significantly to performance degradation of the thermal control surface samples.

Table 2 Error Analysis of α_S Measurements

A. Calorimeter Design Error

Components of Potential Uncertainty in Calorimeter Design	Q Heat Leak Watts	Uncertainty %	Calculating Error ΔQ	$\left(\frac{d\alpha}{dQ}\Delta Q\right)^2$
Support Conductance	0.003	30	0.0009	7.29×10^{-6}
Lead Wire Conductance	0.0044	25	0.0011	10.9
Multilayer Insuation Conductance	0.0003	10	0.0001	0.01
Solar Absorptance in Gap	0.0018	50	0.0009	7.29
Solar Absorptance on AL Teflon	0.0003	50	0.0002	0.04
Temperature Sensor Power Dissipation	0.0015	15	0.0002	0.004
				25.6×10^{-6}

From analysis $\frac{d\alpha}{dQ} \sim = 3.0$

$$\alpha_{S_{Design}} = \left[\sum\left(\frac{d\alpha}{dQ}\Delta Q\right)^2\right]^{0.5} = \pm 0.005$$

RMS ERROR IN ABSOLUTE α_S DUE TO CALORIMETER DESIGN UNCERTAINTY

B. Temperature Calibration Error

From flight data

$$\frac{d\alpha_S}{dT} = 0.0014$$

Calibration curves developed for a $\pm$ 1.0°F maximum error ($\Delta T = \pm 1.0$)

$$\alpha_S \text{ Calibration} = \pm 0.0014$$

C. Temperature Monitor Telemetry Error

From telemetry quantization

$$\Delta T = +1.6^{\circ}F, -0.0^{\circ}F$$

From flight data

$$\frac{d\alpha_S}{dT} = 0.0014$$

$$\alpha_{S\text{Telemetry}} = \left[\left(\frac{d\alpha_S}{dT}\Delta T\right)^2\right]^{0.5} = +0.0022, -0.0$$

D. Conclusion

The calorimeter design errors are essentially negligible when calculating the α_S change over a small temperature range

Absolute α_S Measurement Error	$\Delta\alpha_S$ Measurement Error
+ 0.009	+ 0.004
- 0.006	- 0.001

Table 3 Comparison of Laboratory and Initial Flight Measurements of Solar Absorptance α_s

Sample	Laboratory α_s	Initial Flight α_s
1. 0.002 in. Silver Teflon	0.068	0.068
2. 0.005 in. Aluminized Teflon	0.144	0.140
3. Silica Cloth No. 581	0.197	0.199
4. Silica Cloth No. 581	0.165	0.186
5. 0.002 in. Silver Teflon	0.066	0.076
6. Indium Oxide Coated Mirror	0.082	0.091
7. 0.005 in. Embossed Silver Teflon	0.095	0.094
8. Second Surface Mirror	0.068	0.074
9. ZOT on aluminum (8-10 mil thick)	0.194	0.197
10. ZOT on aluminum (8-10 mil thick)	0.181	0.185
11. Second Surface Mirror	0.068	0.068
12. ZOT on magnesium (8-10 mil thick)	0.188	0.192
13. Second Surface Mirror	0.068	0.065
14. ZOT on aluminum (10-12 mil thick)	0.167	0.177
15. Second Surface Mirror	0.068	0.067
16. ZOT on aluminum (6-7 mil thick)	0.214	0.216
17. Silver-Alumina-Silica	0.158	0.158
18. ZOT on aluminum (10-12 mil thick)	0.167	0.190
19. Second Surface Mirror	0.068	0.076
20. ZOT on magnesium (10-12 mil thick)	0.167	0.199

The primary interest in the calorimeter data is the variation of solar absorptance with time of environmental exposure. When the change in solar absorptance is considered, the uncertainties associated with the calorimeter design become negligible because they are essentially constant over small temperature changes. The temperature monitor calibration error and the telemetry quantization error are still fully involved in the α_s measurement so the final estimated error for measuring the change of solar absorptance with time is +0.004, -0.001 as noted in Table 2.

3.0 Flight Sample Descriptions

The thermal control surface samples evaluated on these calorimeters were selected for their potential application on future spacecraft. Consideration was given to parameters other than thermal performance in the selection process such as weight, cost, complexity of installation and ability to maintain a clean surface. As a result, the materials tested included white paints, silica cloth and metallized Teflon samples as well as the second surface mirrors tested in the early phase of the calorimeter experiment (Reference 1). The detailed description of each of the 20 test samples is given in Table 1 including the method of attaching the sample to the holder.

The laboratory measured values of α_s of these samples are given in Table 3. The laboratory measurements of some sample materials show property variations with temperature and thickness. Figure 7 shows the variation of emissivity with temperature for several of the materials tested in this program. The solar absorptance value of the zinc orthotitanate (ZOT) white paint was shown to vary with thickness from laboratory measurements. Figure 8 shows measurements taken on panels and calorimeter samples coated with ZOT paint of varying thickness.

4.0 Results of Flight Measurements

The flight data values for the solar absorptance of the samples were tabulated and plotted as a function of flight time for periodic comparison with existing data. The data from early flight calorimeters involving primarily second surface mirrors were presented in this manner in Reference 1. Curves of the solar absorptance values of silvered and aluminized Teflon and silica cloth given in Reference 1 are updated in Figure 9.

The solar absorptance flight measurements of representative test samples are shown in Figure 10 as a function of equivalent sun hours and years in orbit. Subsequent curves are given in equivalent sun hours only. The

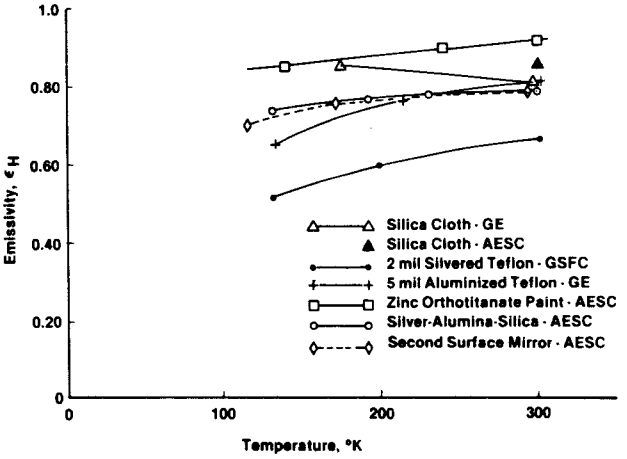

Figure 7 Hemispherical Emittance Versus Temperature For Thermal Control Coatings

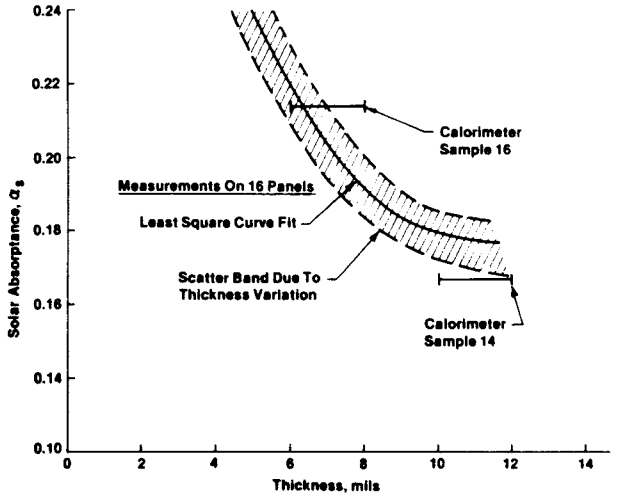

Figure 8 α_s Laboratory Measurements of Zinc Orthotitanate Paint (ZOT)

conversion factor for the satellites is 2400 equivalent sun hours per year. The performance characteristics of each class of material is now analyzed and compared to other flight and laboratory data.

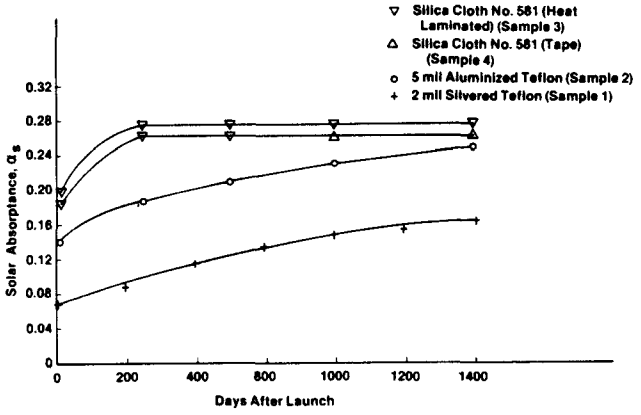

Figure 9 Updated Data For Satellite D (Figure 7 In Reference I)

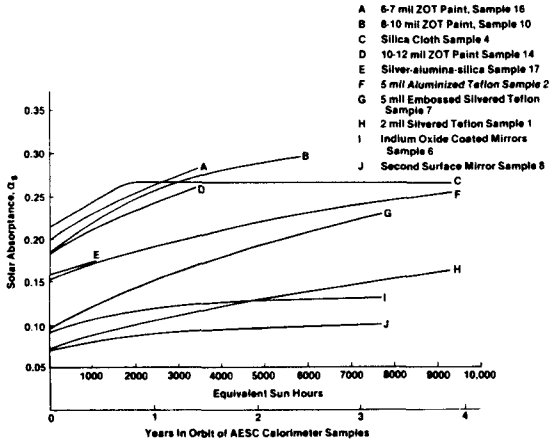

Figure 10 Solar Absorptance Degradation With Time For All Test Sample Types

4.1 Comparative Behavior of Test Samples

4.1.1 Metallized Teflon, α_s

The solar absorptance values for silvered and aluminized Teflon from these calorimeter experiments are plotted in Figure 11 as a function of equivalent sun hours. These samples include two silvered 2 mil thick Teflon samples, an aluminized 5 mil thick Teflon sample, and an embossed silvered 5 mil Teflon sample. This latter sample can be seen in the lower right part of the calorimeter in Figure 1. The aluminized and embossed samples show higher initial α_s values than the plain silvered Teflon samples and the embossed sample shows the highest α_s rise rate with time. The embossed sample was developed to provide flexibility to the surface when large temperature cycles are encountered, but it is apparent that a significant performance penalty is involved. AESC has used 2 mil thick silvered Teflon on sunshades with 300°F (167°C) diurnal temperature swings for several years with no apparent failure.

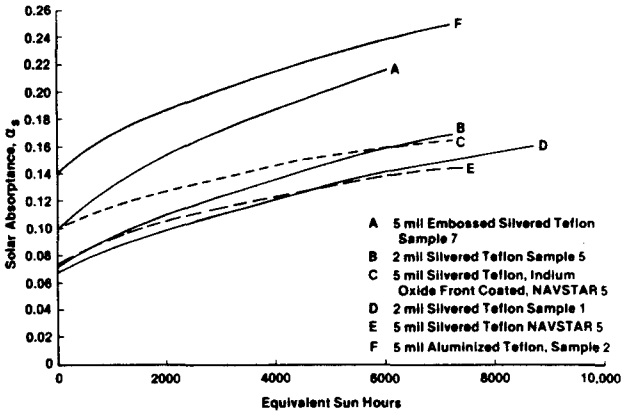

Figure 11 Silvered and Aluminized Teflon

Two samples from the NAVSTAR 5 satellite (Reference 4) are shown in Figure 11. The 5 mil silvered Teflon sample, curve E, has the same general characteristics as the plain AESC silvered Teflon samples. The indium oxide front coated sample shows a higher initial α_s value than the plain silvered Teflon but has the same α_s rise rate with time. This behavior is consistent with the performance of the indium oxide front coated mirror shown in Figure 12.

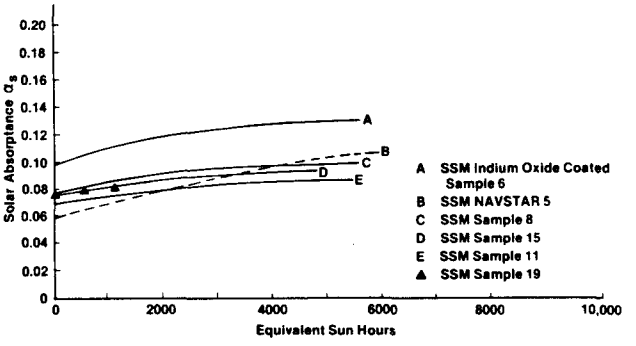

Figure 12 Second Surface Mirrors (SSM)

4.1.2 Second Surface Mirrors, α_s

The second surface mirror samples tested in this phase of the calorimeter experiment were selected primarily as reference surfaces since extensive performance data was obtained in the early phase and reported in Reference 1. The α_s values plotted versus equivalent sun hours in Figure 12 generally follow the data obtained previously for this calorimeter location. Also plotted in Figure 12 for comparison is the second surface mirror data from NAVSTAR 5[4]. The degradation rise rate of α_s as a function of exposure time are comparable for these samples located in clean spacecraft areas. The indium oxide front coated mirror sample shows a higher initial α_s value but its rise rate with exposure is similar to other mirror samples. This behavior is similar to that experienced for the indium oxide front coated silvered Teflon sample on NAVSTAR 5 shown in Figure 11. The indium oxide coated mirror sample is seen as the lower left sample on the calorimeter shown in Figure 1. An analysis of the sample indicates that a significant part of the increased initial α_s value over the conventional mirror samples can be attributed to the solder grounding tabs that can be seen in Figure 1.

4.1.3 Silica Cloth, α_s

The two test samples of silica cloth have an initial high α_s rise rate as shown in Figure 13 but level off after about 2000 hours of sun exposure and remain constant through the rest of the measured flight. Comparative flight data from SCATHA[9] spacecraft are also shown in Figure 13.

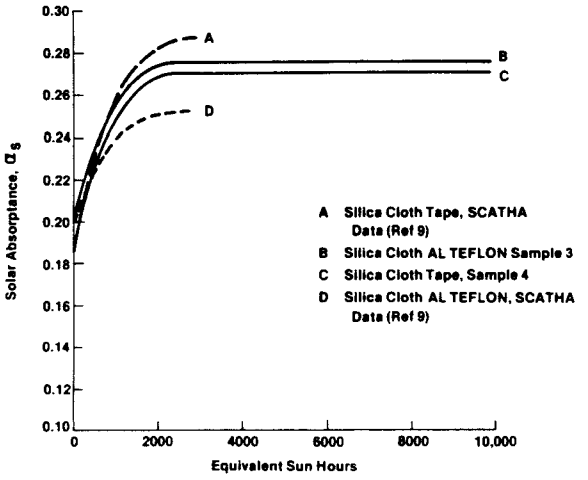

Figure 13 Silica Cloth α_s Degradation With Time

4.1.4 White Paint, α_s

Curves of solar absorptance versus equivalent sun hours of exposure for the seven zinc orthotitanate samples are shown in Figure 14. These samples have different thicknesses, varying from 6-7 mils up to 10-12 mils, and show the decrease in initial solar absorptance with increase in thickness as was demonstrated with the laboratory data in Figure 8. The existence of the apparent discrepancy in the dependence on thickness of curves C and D (samples 18 and 20) is not yet determined as the data is preliminary. All samples do, however, show comparable rates of solar absorptance degradation indicating the lack of a dependence of the α_s degradation rate on sample thickness. Three 8-10 mil samples were tested, one on a magnesium substrate (curve E) and two on aluminum (curves F and G). Although the difference is not large, the magnesium substrate sample has a α_s degradation rate greater than those on aluminum. This discrepancy lies outside the error band for α_s. The reason for this difference is not yet known, but as all three samples were tested on the same flight it cannot be explained by differences in their space environment. In addition to the substrate difference, their surfaces were prepared differently but the effect of this has not been resolved.

Also shown in Figure 14 are data on white paint S13G/Lo from NAVSTAR 6 (Reference 4). The initial values of α_s for ZOT and S13G/LO are comparable, however the degradation rate and asymptotic α_s, for S13G/LO is substantially greater than for all ZOT samples.

4.1.5 Silver-Alumina-Silica, α_s

A sample of vapor deposited silver-alumina-silica (SAS) on aluminum was flight tested and the solar absorptance α_s change with time is shown in Figure 15. Also shown for comparison are two representative curves for second surface mirrors and ZOT paint. The SAS sample was prepared following the specifications given in Table 4 which was developed from information provided in References 5, 6, and 7. The aluminum oxide overcoat was 22 quarter wavelengths thick while the silicon dioxide film was 6 quarter wavelengths thick. The initial solar absorptance value lies between those of second surface mirrors and white paint and similarly the preliminary data shows the α_s degradation rate for SAS is larger than for second surface mirrors but less than that of white paint indicating that it may be an acceptable thermal control coating for some applications. Lower α_s values may be expected from improved fabrication control in view of the information in the above references.

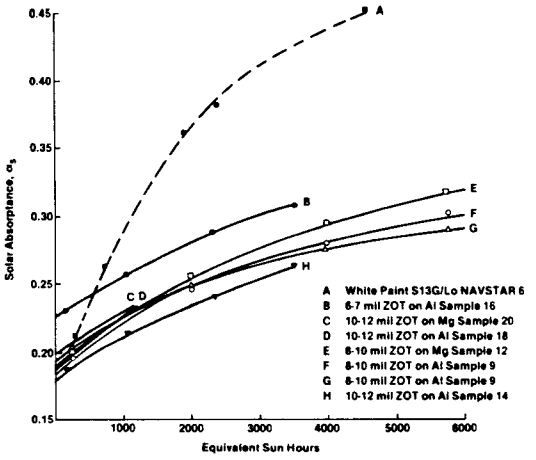

Figure 14 White Paint

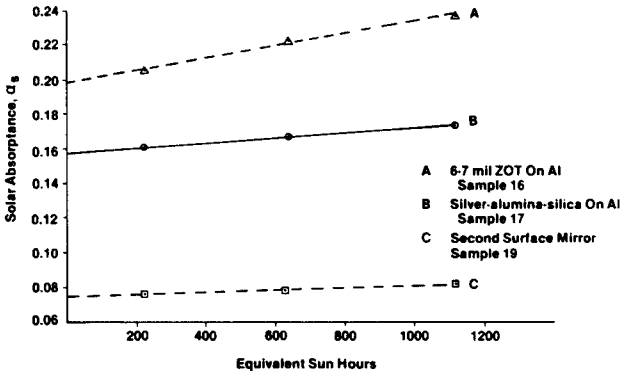

Figure 15 Silver-Alumina-Silica

Table 4 Surface Layers of Silver-Alumina-Silica

Layer 4 -	SiO_2, 825 + 84 nm,-0 nm
Layer 3 -	AL_2O_3, 3025 + 275 nm,-0 nm
Layer 2 -	OPAQUE SILVER, 90 ± 10 nm DEPOSITION RATE, 10-20 nm/sec
Layer 1 -	DIFFUSION BARRIER AL_2O_3 100 ± 10 nm
Substrate -	ALUMINUM

4.1.6 Measurements of Emissivity

The data on solar absorptance presented above was obtained from flight measurements that were reduced assuming no change in the emissivity with time of the thermal control surface under investigation. Throughout the life of this calorimeter experiment program several evaluations were made on different samples to validate this assumption. This was done by comparing the minimum diurnal temperature when the sample was shaded from the sun with the computed predicted value over a one year period with an assumption of a constant emissivity. Figure 16 shows that the measured change in minimum temperature with time over a 1 year period was matched well with the predicted temperature change assuming a constant emissivity.

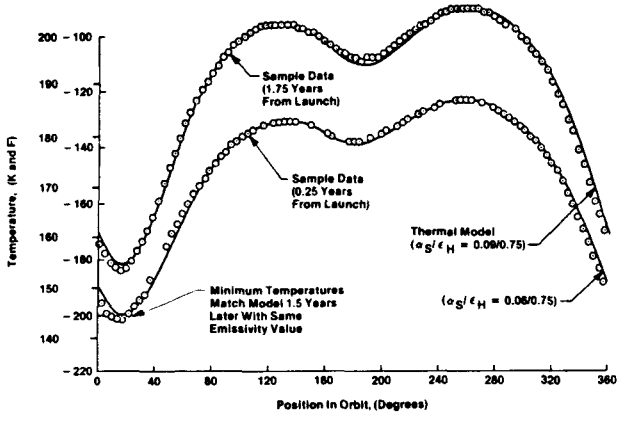

Figure 16 Comparison of Minimum Diurnal Temperatures 1.5 Years Apart With Computer Model Having Constant Emissivity[1]

The value of emissivity of some thermal control surfaces does vary with temperature. Laboratory measurements made on the thermal control surface materials used in this experimental program are plotted in Figure 7.

4.2 Development of Design Working Equations

Data on the degradation of thermal control surfaces on several orbital spacecraft have been presented in the literature. However, because of the diverse spacecraft configurations and the different thermal test surface locations relative to contamination sources, it is difficult to compile these data into a usable design source for spacecraft thermal control systems. The data developed in this calorimeter experimental program evaluated several types of thermal control surfaces in a clean location on a synchronous orbiting satellite. These data can provide a reliable design baseline for thermal control radiator surfaces on long-life satellites.

To be most useful for design applications the measured solar absorptance data were converted into equivalent sun hours of exposure. The data used to plot the flight measurement results given in Figures 10 thru 14 were entered into a computer program that produced the coefficients of the exponential equation

$$\alpha_s = \alpha_o + (\alpha_m - \alpha_o)(1 - e^{-t/\tau}) \qquad (1)$$

which gives the value of solar absorptance α_s as a function of equivalent sun hours. These coefficents are given in Table 5. To achieve a suitable curve fit over the long-life performance of most of these surfaces it was necessary to eliminate the first flight measurement. This was

Table 5 Solar Absorptance (α_s) and Emissivity (ϵ) Data

$$\alpha_s = \alpha_o + (\alpha_m - \alpha_o)(1 - e^{-t/\tau})$$

α_o = initial value α_m = asymptotic value

Flight Sample	Surface Type	α_o	α_m	τ (ESH)	Emissivity* (ϵ)	Range (Max ESH)
1.	0.002-in Silvered Teflon	0.080	0.241	12123	0.66	9300
2.	0.005-in Aluminized Teflon	0.163	0.316	9525	0.80	9300
3.	Silica cloth No. 581	$\alpha_s = 0.224 + 3.03 \times 10^{-5}t$			0.86	<1800
		$\alpha_s = 0.273$				>1800
4.	Silica cloth No. 581	$\alpha_s = 0.213 + 2.97 \times 10^{-5}t$			0.86	<1800
		$\alpha_s = 0.267$				>1800
5.	0.002-in Silvered Teflon	0.085	0.246	8769	0.66	7700
6.	Indium Oxide Coated Mirrors	0.096	0.133	2265	0.79	7700
7.	0.005-in Embossed Ag Teflon	0.108	0.297	7467	0.80	7700
8.	Second Surface Mirrors	0.077	0.103	3138	0.79	7700
9.	ZOT paint (8-10 mil thick)	0.198	0.301	2863	0.91	5800
10.	ZOT paint (8-10 mil thick)	0.185	0.314	2933	0.91	5800
11.	Second Surface Mirrors	$\alpha_s = 0.069 + 1.5 \times 10^{-6}t$			0.79	5800
12.	ZOT paint (8-10 mil thick)	0.192	0.350	3836	0.91	5800
13.	Second Surface Mirror	$\alpha_s = 0.755 + 4.7 \times 10^{-6}t$			0.79	3400
14.	ZOT paint (10-12 mil thick)	0.188	0.358	5920	0.91	3400
15.	Second Surface Mirror	0.079	0.109	6259	0.79	3400
16.	ZOT paint (6-7 mil thick)	0.230	0.405	5757	0.91	3400
17.	Silver-Alumina-Silica	$\alpha_s = 0.156 + 1.50 \times 10^{-5}t$**			0.79	1100
18.	ZOT paint (10-12 mil thick)	$\alpha_s = 0.190 + 3.65 \times 10^{-5}t$**			0.91	1100
19.	Second Surface Mirrors	$\alpha_s = 0.075 + 6.1 \times 10^{-6}t$**			0.79	1100
20.	ZOT paint (10-12 mil thick)	$\alpha_s = 0.199 + 3.09 \times 10^{-5}t$**			0.91	1100

* Emissivity values at ~295K (see Figure 7 for ϵ vs temp)
** Preliminary data

caused by the generally sharp change in degradation rate after several months of flight. The curves in Figure 10 thru 14 have been drawn with the initial values fitted in but the equations without the first point will give a greater error of up to +0.005 for the first 400 equivalent sun hours of exposure.

5.0 Application of Data

Passive radiators are the primary method of temperature control for operating equipment and experiments on orbiting spacecraft. Most satellite experiments and operating equipment must be maintained within a given temperature range over its operating life. These temperatures are determined by qualification tests and by reliability derating values when long-life is involved. These temperature specifications along with the heat loads and available radiator surface orientation are required to begin the radiator design analysis.

In addition to the heat generated by the equipment, the heat absorbed by the radiator from the Sun, from earth emission, and from the spacecraft itself must be rejected. This aspect of passive radiator design and performance is controlled only by the selection of the thermal control surface properties. (Louvers and other devices to block the sun from the radiator surface are considered to be active devices.) To minimize the influence of solar heat on the radiator performance, a low value of solar absorptance is desired. To minimize the size and weight of a radiator, a high value of emissivity is desired. Thermal control surfaces developed for spacecraft application have had, as their goal, a low value of solar absorptance and a high value of emissivity in the range of infrared wavelength.

The long-life aspects of the thermal performance analysis is dependent on the degraded values of the radiator surface properties. The thermal control surface properties in this experiment were evaluated in a clean location. In the presence of contamination however, higher degradation rates will be experienced and adjustments must be made to the "clean" degradation rates. At present, the influence of contamination has not been adequately quantified for design purposes but efforts are being intensified in this area as a result of the Shuttle Transportation System studies.[11,12]

The performance analysis of a passive radiator for a spacecraft application initially involves two steps. The first step is to screen the potential thermal control surfaces and select a few that can be examined in more detail. This will establish the predicted performance diurnally and with time in orbit. The screening is accomplished under steady-state conditions to ascertain the average operating temperature, and to approximate the the maximum and minimum diurnal temperatures.

The equation for calculating the radiator temperature under steady-state conditions is

$$T = \frac{1}{\epsilon \sigma A}(\alpha_s E_s + \alpha_s E_a + E_e + Q)^{1/4} \qquad (2)$$

where direct solar heat load is given by

$$E_s = S_o A (\cos\theta), \qquad (3)$$

θ = angle between surface normal and sun line

albedo heat load is given by

$$E_a = a S_o F_a, \qquad (4)$$

earthshine heat load is given by

$$E_e = H_e F_e, \qquad (5)$$

and Q = heat load from component or experiment.

The geometrical radiator orientation factors in the above equations F_a, F_e, and the heat loads from earthshine and albedo can be obtained from spacecraft design manuals and handbooks such as Reference 8.

The prediction of diurnal temperatures of a passively cooled device on a spacecraft requires that a transient analysis be made to account for the heat capacitance in the system. The basic equation for conducting a transient analysis is

$$T_2 = T_1 + \frac{\Delta t}{C}(\alpha_s E_s + \alpha_s E_a + E_e + Q_1 - \sigma \epsilon A T_1^4) \qquad (6)$$

The radiator surface values of α_s and ϵ play a major role in predicting the radiator temperature and in the design of spacecraft thermal control systems as seen from equations (2) and (6). The life degraded values of α_s are required to predict realistic long-life thermal performance characteristics of satellites.

6.0 Conclusions

The performance data presented above is comprised of a unique group of different types of thermal control surfaces exposed to the same long-life orbital environment. Direct comparison of the tested surface samples to each other is made practical by the use of similar reference samples on each of the satellites. The use of an efficient calorimeter that thermally isolates the test samples from the spacecraft provides accurate and reliable results. As a consequence the data compilation presented above forms a reliable design baseline for thermal control of satellite systems.

This baseline data is referenced to a clean (non-contaminated) surface in an geosynchronous orbit. Where surface contamination is expected from the spacecraft, adjustments must be made to the "clean" degradation rates presented in this paper. The technology for selection of contamination factors as a function of surface material, temperature, location and time is only now being seriously investigated. When the contamination correction factor is adequately developed quantitatively, its application in conjunction with the above "clean" baseline data will provide engineers the complete tools necessary for design of reliable, long-life thermal control systems for satellites.

References

1. Curran D.G.T., and Millard J.M., "Results of Contamination/Degradation Measurements on Thermal Control Surfaces of an Operational Satellite", AIAA 12th Thermophysics Conference, Albuquerque, N.M., AIAA Paper No. 77-740, June 27-29, 1977

2. Rajagopalan R. and Willson V.J., "Thermal Performance of Anik-B Satellite in Orbit", AIAA 15th Thermophysics Conference, July 14-16, 1980, Snowmass, Colorado, AIAA Paper No. 80-1498.

3. Bouchez J.P. and Howle D., "The Orbital Test Satellite (OTS) Thermal Experience After 3.5 Years in Orbit", AIAA/ASME 3rd Joint Thermophysics Fluids, Plasma and Heat Transfer Conference, June 7-11, 1982, St. Louis, Missouri.

4. Pence W.R. and Grant T.J., " α_s Measurements of Thermal Control Coatings on NAVSTAR Global Positioning System Spacecraft", AIAA 16th Thermal Physics Conference, Palo Alto, California June 23, 1981.

5. Haas G., Heaney J.B., and Triolo J.J., "Evaporated Ag coated with Double Layers of Al_2O_3 and Silicon Oxide to Produce Surface Films with Low Solar Absorptivity and High Emissivity", Optics Communications, Vol. 8, No. 3, July 1973, Page 183.

6. Haas G., Ramsey J.B., Heaney J.B., and Triolo, J.J., "Reflectance, Solar Absorptivity and Thermal Emissivity of S_1O_2 - Coated Aluminum", Applied Optics Vol. 8, No. 2, February 1969, Page 275.

7. Haas G., Ramsey J.B. Heaney J.B., and Triolo J.J., "Thermal Emissivity and Solar Absorptivity of Aluminum Coated with Double Layer of Aluminum Oxide and Silicon Oxide", Applied Optics, Vol. 10, No. 6, June 1971, Page 1296.

8. Donabedian M., Chapter 15, The Infrared Handbook, Office of Naval Research, 1978.

9. Hall D. F. and Fote A.A. " α_s/ϵ Measurements of Thermal Control Coatings on the P78-2 (SCATHA) Spacecraft", AIAA 15th Thermophysics Conference, July 14-16, 1980, Snowmass, Colorado.

10. Lockerby S.C., Barsh M.K., and Mossman D.L. "ZOT-A White Thermal Control Coating for Space Environment: Considerations", National SAMPE Technical Conference Series, Vol. 14, pp. 49-51, 1982.

11. Barnhart B.J. and Balse, J.C., "Shuttle Contamination and Experimentation: DOD Implications", SPIE, Proceedings Vol. 280, Pg. 127, 1981.

12. Various authors, Spacecraft Contamination Environment session, SPIE Proceedings Vol. 338, May 1982.